Neutron Star Interiors and the Equation of State of Superdense Matter

Fridolin Weber[1], Rodrigo Negreiros[2], and Philip Rosenfield[3]

[1] San Diego State University fweber@sciences.sdsu.edu
[2] San Diego State University negreiro@sciences.sdsu.edu
[3] San Diego State University philrose@sciences.sdsu.edu

Summary. Neutron stars contain matter in one of the densest forms found in the Universe. This feature, together with the unprecedented progress in observational astrophysics, makes such stars superb astrophysical laboratories for a broad range of exciting physical studies. This paper gives an overview of the phases of dense matter predicted to make their appearance in the cores of neutron stars. Particular emphasis is put on the role of strangeness. Net strangeness is carried by hyperons, K-mesons, H-dibaryons, and strange quark matter, and may leave its mark in the masses, radii, moment of inertia, dragging of local inertial frames, cooling behavior, surface composition, and the spin evolution of neutron stars. These observables play a key role for the exploration of the phase diagram of dense nuclear matter at high baryon number density but low temperature, which is not accessible to relativistic heavy ion collision experiments.

1 Introduction

Neutron stars are dense, neutron-packed remnants of stars that blew apart in supernova explosions. Many neutron stars form radio pulsars, emitting radio waves that appear from the Earth to pulse on and off like a lighthouse beacon as the star rotates at very high speeds. Neutron stars in x-ray binaries accrete material from a companion star and flare to life with a burst of x-rays. The most rapidly rotating, currently known neutron star is pulsar PSR J1748-2446ad, which rotates at a period of 1.39 ms (which corresponds to a rotational frequency of 719 Hz) [1]. It is followed by PSRs B1937+21 [2] and B1957+20 [3] whose rotational periods are 1.58 ms (633 Hz) and 1.61 ms (621 Hz), respectively. Finally, the recent discovery of X-ray burst oscillations from the neutron star X-ray transient XTE J1739–285 [4] could suggest that XTE J1739–285 contains the most rapidly rotating neutron star yet discovered. Measurements of radio pulsars and neutron stars in x-ray binaries comprise most of the neutron star observations. Improved data on isolated neutron stars (e.g. RX J1856.5-3754, PSR 0205+6449) are now becoming available, and future investigations at gravitational wave observatories focus on neutron

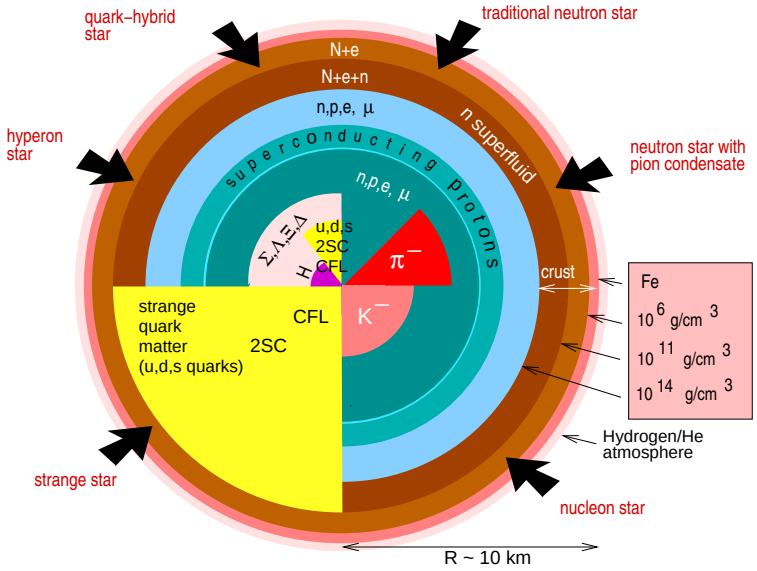

Fig. 1. Neutron star compositions predicted by theory.

stars as major potential sources of gravitational waves (see [5] for a recent overview). Depending on star mass and rotational frequency, the matter in the core regions of neutron stars may be compressed to densities that are up to an order of magnitude greater than the density of ordinary atomic nuclei. This extreme compression provides a high-pressure environment in which numerous subatomic particle processes are likely to compete with each other [6, 7]. The most spectacular ones stretch from the generation of hyperons and baryon resonances ($\Sigma, \Lambda, \Xi, \Delta$), to quark ($u, d, s$) deconfinement, to the formation of boson condensates (π^-, K^-, H-matter) [6, 7, 8, 9, 11, 12] (see Fig. 1). In the framework of the strange matter hypothesis [15, 16, 17], it has also been suggested that 3-flavor strange quark matter–made of absolutely stable u, d, and s quarks–may be more stable than ordinary atomic nuclei. In the latter event, neutron stars should in fact be made of such matter rather than ordinary (confined) hadronic matter [18, 19, 20]. Another striking implication of the strange matter hypothesis is the possible existence of a new class of white-dwarfs-like strange stars (strange dwarfs) [21]. The quark matter in neutron stars, strange stars, or strange dwarfs ought to be in a color superconducting state [22, 23, 24, 25]. This fascinating possibility has renewed tremendous interest in the physics of neutron stars and the physics and astrophysics of (strange) quark matter [11, 22, 23]. This paper discusses the possible phases of ultra-dense nuclear matter expected to exist deep inside neutron stars and reviews selected models derived for the equation of state (eos) of such matter (see also [6, 7, 8, 9, 10, 11, 12, 13, 14]).

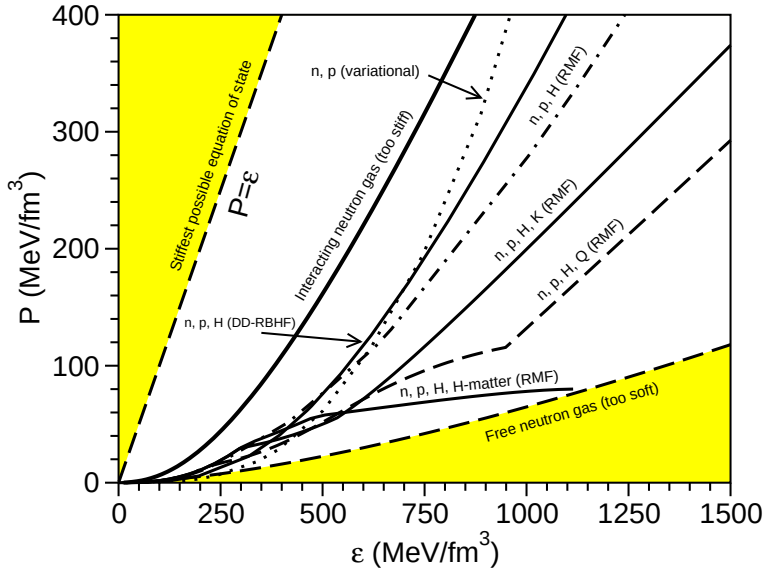

Fig. 2. Models for the equation of state (pressure versus energy density) of neutron star matter [11]. The notation is as follows: RMF=relativistic mean-field model; DD-RBHF=density dependent relativistic Brueckner-Hartree-Fock model; n=neutrons; p=protons; H=hyperons, K=$K^-[u,\bar{s}]$ meson condensate; Q=u,d,s quarks; H-matter=H-dibaryon condensate.

2 Neutron Star Masses

In 1939, Tolman, Oppenheimer and Volkoff performed the first neutron star calculations, assuming that such objects are entirely made of a gas of non-interacting relativistic neutrons [26, 27]. The eos of such a gas is extremely soft, i.e. very little additional pressure is gained with increasing density, as can be seen from Fig. 2, and predicts a maximum neutron star mass of just 0.7 $M_\odot$ (Fig. 3) at an unrealistically high density of 17 times the density of nuclear matter (Fig. 4). It is interesting to note that the inclusion of interactions among the neutrons increases the star's maximum mass from 0.7 $M_\odot$ to around 3 $M_\odot$ (Figs. 3 and 4). However, the radii of the latter are so big that mass shedding from the star's equator occurs at rotational frequencies that are considerably smaller than those observed for PSR J1748-2446ad, 716 Hz (1.39 ms) [1], or B1937+21, 630 Hz (1.58 ms) [2]. An interacting neutron gas thus fails to accommodate the observed rapidly rotating neutron stars. The other extreme, a non-interacting relativistic neutron gas, fails too since it does not accommodate the Hulse-Taylor pulsar ($M = 1.44\,M_\odot$) [28], and also conflicts with the average neutron star mass of $1.350 \pm 0.004\,M_\odot$ derived by Thorsett and Chakrabarty [29] from observations of radio pulsar systems. More than that, recent observations

indicate that neutron star masses may be as high as around 2 $M_\odot$. Examples of such very heavy neutron stars are $M_{\rm J0751+1807} = 2.1 \pm 0.2\ M_\odot$ [30], $M_{\rm 4U\,1636+536} = 2.0 \pm 0.1\ M_\odot$ [31], $M_{\rm Vela\,X-1} = 1.86 \pm 0.16\, M_\odot$ [32], $M_{\rm Cyg\,X-2} = 1.78 \pm 0.23\, M_\odot$ [33, 34]. Large masses have also been reported for the high-mass x-ray binary 4U 1700–37 and the compact object in the low-mass x-ray binary 2S0921–630, $M_{\rm 4U\,1700-37} = 2.44 \pm 0.27\ M_\odot$ [35] and $M_{\rm 2S0921-630} = 2.0 - 4.3 M_\odot$ [36]. respectively. The latter two objects may be either massive neutron stars or low-mass black holes with masses slightly higher than the maximum possible neutron star mass of $\sim 3 M_\odot$. This value follows from a general, theoretical estimate of the maximal possible mass of a stable neutron star as performed by Rhoades and Ruffini [37] on the basis that (1) Einstein's theory of general relativity is the correct theory of gravity, (2) the eos satisfies both the microscopic stability condition $\partial P/\partial\epsilon \geq 0$ and the causality condition $\partial P/\partial\epsilon \leq c^2$, and (3) that the eos below some matching density is known. From these assumptions, it follows that the maximum mass of the equilibrium configuration of a neutron star cannot be larger than $3.2\, M_\odot$. This value increases to about $5\, M_\odot$ if one abandons the causality constraint $\partial P/\partial\epsilon \leq c^2$ [38, 39], since it allows the eos to behave stiffer at asymptotically high nuclear densities. If either one of the two objects 4U 1700–37 or 2S0921–630 were a black hole, it would confirm the prediction of the existence of low-mass black holes [40]. Conversely, if these objects were massive neutron stars, their high masses would severely constrain the eos of dense nuclear matter.

3 Composition of Cold and Dense Neutron Star Matter

A vast number of models for the equation of state of neutron star matter has been derived in the literature over the years. These models can roughly be classified as follows:

- Thomas-Fermi based models [41, 42]
- Schroedinger-based models (e.g. variational approach, Monte Carlo techniques, hole line expansion (Brueckner theory), coupled cluster method, Green function method) [8, 43, 44, 45, 46, 47, 48]
- Relativistic field-theoretical treatments (relativistic mean field (RMF), Hartree-Fock (RHF), standard Brueckner-Hartree-Fock (RBHF), density dependent RBHF (DD-RBHF) [49, 50, 51, 52, 53, 54]
- Nambu-Jona-Lasinio (NJL) models [55, 56, 57, 58, 59, 60]
- Chiral SU(3) quark mean field model [61].

A collection of equations of state computed for several of these models is shown in Fig. 2. Mass–radius relationships of neutron stars based on these equations of state are shown in Fig. 3. Any acceptable nuclear many-body calculation must correctly reproduce the bulk properties of nuclear matter at saturation density, $n_0 = 0.16$ fm^{-3}. These are the binding energy, $E/A = -16.0$ MeV,

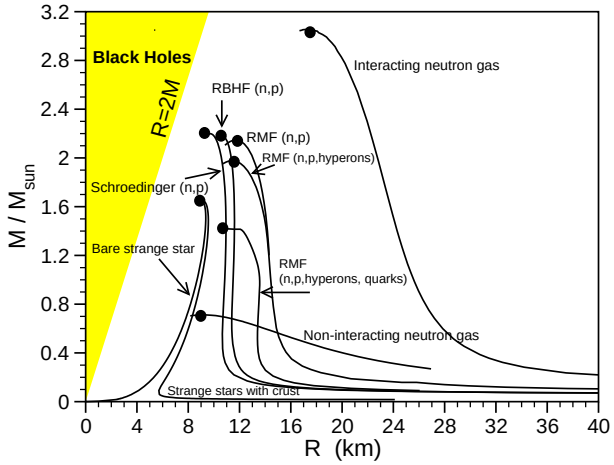

Fig. 3. Mass-radius relationship of neutron stars and strange stars [11]. The strange stars may be enveloped in a crust of ordinary nuclear material whose density is below neutron drip density [18, 62, 63].

effective nucleon mass, $m_{\rm N}^* = 0.79\, m_{\rm N}$, incompressibility, $K \simeq 240$ MeV, and the symmetry energy, $a_{\rm s} = 32.5$ MeV.

3.1 Hyperons and baryon resonances

At the densities in the interior of neutron stars, the neutron chemical potential, μ^n, is likely to exceed the masses, modified by interactions, of Σ, Λ and possibly Ξ hyperons [64]. Hence, in addition to nucleons, neutron star matter may be expected to contain significant populations of strangeness carrying hyperons. The thresholds of the lightest baryon resonances ($\Delta^-, \Delta^0, \Delta^+, \Delta^{++}$) are not reached in relativistic mean-field (Hartree) calculations. This is different for many-body calculations performed at the relativistic Brueckner-Hartree-Fock level, where Δ's appear very abundantly [65]. In any event, pure neutron matter constitutes an excited state relative to hyperonic matter which, therefore, would quickly transform via weak reactions like

$$n \rightarrow p + e^- + \bar{\nu}_e \tag{1}$$

to the lower energy state. The chemical potentials associated with reaction (1) in equilibrium obey the relation

$$\mu^n = \mu^p + \mu^{e^-}\,, \tag{2}$$

where $\mu^{\bar{\nu}_e} = 0$ since the mean free path of (anti) neutrinos is much smaller than the radius of neutron stars. Hence (anti) neutrinos do not accumulate inside neutron stars. This is different for hot proto-neutron stars [66]. Equation (2) is a special case of the general relation

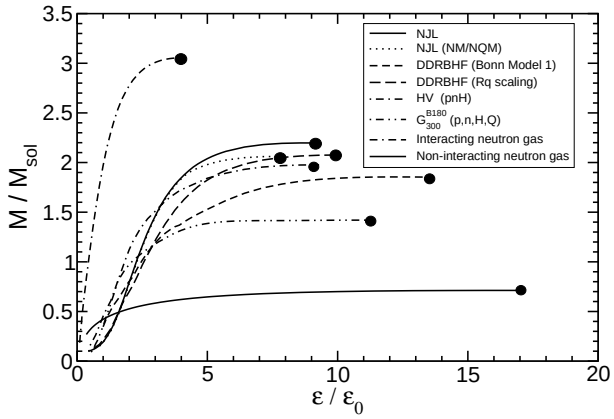

Fig. 4. Neutron star mass versus central density (in units of nuclear matter density, $\epsilon_0 = 140$ MeV/fm^3).

$$\mu^{\chi} = B^{\chi}\mu^{n} - q^{\chi}\mu^{e^-} \,, \tag{3}$$

which holds in any system characterized by two conserved charges. These are in the case of neutron star matter electric charge, q^{χ}, and baryon number charge, B^{χ}. Application of Eq. (3) to the Λ hyperon ($B^{\Lambda} = 1$, $q^{\Lambda} = 0$), for instance, leads to

$$\mu^{\Lambda} = \mu^{n} \,. \tag{4}$$

Ignoring particle interactions, the chemical potential of a relativistic particle of type χ is given by

$$\mu^{\chi} = \omega(k_{F_\chi}) \equiv \sqrt{m_\chi^2 + k_{F_\chi}^2} \,, \tag{5}$$

where $\omega(k_{F_\chi})$ is the single-particle energy of the particle and k_{F_χ} its Fermi momentum. Substituting (5) into (4) leads to

$$k_{F_n} \geq \sqrt{m_\Lambda^2 - m_n^2} \simeq 3 \text{ fm}^{-1} \Rightarrow n \equiv \frac{{k_{F_n}}^3}{3\pi^2} \simeq 6 n_0 \,, \tag{6}$$

where $m_\Lambda = 1116$ MeV and $m_n = 939$ MeV was used. That is, if interactions among the particles are ignored, neutrons are replaced with Λ's in neutron star matter at densities of around six times the density of nuclear matter. This value is reduced to about $2\,n_0$ by the inclusion of particle interactions [64]. Densities that small are easily reached in the cores of neutron stars. Hence, in addition to nucleons and electrons, neutron stars may be expected to contain considerable populations of strangeness-carrying Λ hyperons, possibly accompanied by smaller populations of the charged states of the Σ and Ξ hyperons [64]. Depending on the star's mass, the total hyperon population can be very large [64], which is illustrated graphically in Figs. 5 and 6 for

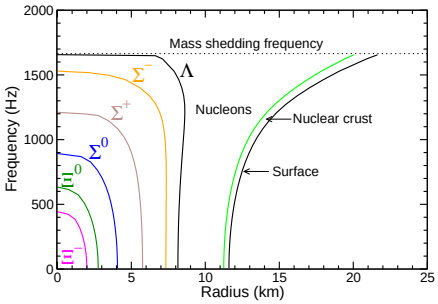

Fig. 5. Hyperon composition of a rotating neutron star in equatorial direction.

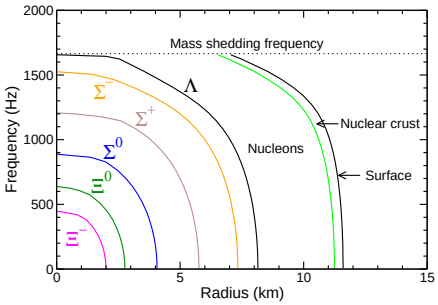

Fig. 6. Same as Fig. 5, but in polar direction.

rotating neutron stars whose equation of state is computed in the framework of the relativistic DD-RBHF formalism [52]. Aside from chemical equilibrium, the condition of electric charge neutrality of neutron star matter,

$$\sum_{\chi=p,\Sigma^{\pm},\Xi^{-},\Delta^{++},\ldots;e^{-},\mu^{-}} q^{\chi}\, k_{F_\chi}^3 \;+\; 3\,\pi^2\, n^M\, \Theta(\mu^M - m_M) \equiv 0\,, \qquad (7)$$

where M stands for π^- or K^- mesons, plays a key role for the particle composition of neutron star matter too. The last term in (7) accounts for the possible existence of either a π^- or a K^- meson condensate in neutron star matter, which will be discussed in more detail in Sect. 3.2. Before, however, we illustrate the importance of Eqs. (2) and (7) for the proton-neutron fraction of neutron star matter. The beta decay and electron capture processes among nucleons, $n \to p + e^- + \bar{\nu}_e$ and $p + e^- \to n + \nu_e$ respectively, also known as nucleon direct Urca processes, are only possible in neutron star matter if the proton fraction exceeds a certain critical value [67]. Otherwise energy and momentum can not be conserved simultaneously for these reactions so that they are forbidden. For a neutron star made up of only nucleons and electrons, it is rather straightforward to show that the critical proton fraction is around 11%. This follows from $\mathbf{k}_{F_n} = \mathbf{k}_{F_p} + \mathbf{k}_{F_e}$ combined with the condition of electric charge neutrality of neutron star matter. The triangle inequality then requires for the magnitudes of the particle Fermi momenta $k_{F_n} \leq k_{F_p} + k_{F_e}$, and charge neutrality dictates that $k_{F_p} = k_{F_e}$. Substituting $k_{F_p} = k_{F_e}$ into the triangle inequality leads to $k_{F_n} \leq 2k_{F_p}$ so that for the particle number densities of neutrons and protons $n_n \leq 8n_p$. Expressed as a fraction of the system's total baryon number density, $n \equiv n_p + n_n$, one thus arrives at $n_p/n > 1/9 \simeq 0.11$, which is the figure quoted just above. Medium effects and interactions among the particles modify this value only slightly but the presence of muons raises it to about 0.15. Hyperons, which may exist in neutron star matter rather abundantly, produce neutrinos via direct Urca processes like $\Sigma^- \to \Lambda + e^- + \bar{\nu}_e$ and $\Lambda + e^- \to \Sigma^- + \nu_e$ [68]. The direct Urca processes are of key importance for neutron star cooling (see D. Page's

contribution elsewhere in this volume). In most cases, the nucleon direct Urca process is more efficient than the ones involving hyperons [69, 70].

3.2 Meson condensation

The condensation of negatively charged mesons in neutron star matter is favored because such mesons would replace electrons with very high Fermi momenta. Early estimates predicted the onset of a negatively charged pion condensate at around $2n_0$ (see, for instance, Ref. [71]). However, these estimates are very sensitive to the strength of the effective nucleon particle-hole repulsion in the isospin $T = 1$, spin $S = 1$ channel, described by the Landau Fermi-liquid parameter g', which tends to suppress the condensation mechanism. Measurements in nuclei tend to indicate that the repulsion is too strong to permit condensation in nuclear matter [72, 73]. In the mid 1980s, it was discovered that the in-medium properties of $K^-[u\bar{s}]$ mesons may be such that this meson rather than the π^- meson may condense in neutron star matter [74, 75, 76].

The condensation is initiated by the schematic reaction $e^- \rightarrow K^- + \nu_e$. If this reaction becomes possible in neutron star matter, it is energetically advantageous to replace the fermionic electrons with the bosonic K^- mesons. Whether or not this happens depends on the behavior of the K^- mass, $m^*_{K^-}$, in neutron star matter. Experiments which shed light on the properties of the K^- in nuclear matter have been performed with the Kaon Spectrometer (KaoS) and the FOPI detector at the heavy-ion synchrotron SIS at GSI [77, 78, 79, 80, 81]. An analysis of the early K^- kinetic energy spectra extracted from Ni+Ni collisions [77] showed that the attraction from nuclear matter would bring the K^- mass down to $m^*_{K^-} \simeq 200$ MeV at densities $\sim 3\,n_0$. For neutron-rich matter, the relation $m^*_{K^-}/m_{K^-} \simeq 1 - 0.2n/n_0$ was established [82, 83, 84], with $m_K = 495$ MeV the K^- vacuum mass. Values of around $m^*_{K^-} \simeq 200$ MeV may be reached by the electron chemical potential, μ^e, in neutron star matter [7, 64] so that the threshold condition for the onset of K^- condensation, $\mu^e = m^*_K$ might be fulfilled for sufficiently dense neutron stars, provided other negatively charged particles (Σ^-, Δ^-, d and s quarks) are not populated first and prevent the electron chemical potential from increasing with density.

We also note that K^- condensation allows the conversion reaction $n \rightarrow p + K^-$. By this conversion the nucleons in the cores of neutron stars can become half neutrons and half protons, which lowers the energy per baryon of the matter [85]. The relative isospin symmetric composition achieved in this way resembles the one of atomic nuclei, which are made up of roughly equal numbers of neutrons and protons. Neutron stars are therefore referred to, in this picture, as nucleon stars. The maximum mass of such stars has been calculated to be around $1.5\,M_\odot$ [86]. Consequently, the collapsing core of a supernova, e.g. 1987A, if heavier than this value, should go into a black hole rather than forming a neutron star, as pointed out by Brown et al. [40, 82, 83].

This would imply the existence of a large number of low-mass black holes in our galaxy [40]. Thielemann and Hashimoto [87] deduced from the total amount of ejected ^{56}Ni in supernova 1987A a neutron star mass range of $1.43 - 1.52\ M_\odot$. If the maximum neutron star mass should indeed be in this mass range ($\sim 1.5\ M_\odot$), the existence of heavy neutron stars with masses around 2 $M_\odot$ (Sect. 2) would be ruled out. Lastly, we mention that meson condensates lead to neutrino luminosities which are considerably enhanced over those of normal neutron star matter. This would speed up neutron star cooling considerably [86, 70].

3.3 H-matter and exotic baryons

A novel particle that could be of relevance for the composition of neutron star matter is the H-dibaryon (H=($[ud][ds][su]$)), a doubly strange six-quark composite with spin and isospin zero, and baryon number two [88]. Since its first prediction in 1977, the H-dibaryon has been the subject of many theoretical and experimental studies as a possible candidate for a strongly bound exotic state. In neutron star matter, which may contain a significant fraction of Λ hyperons, the Λ's could combine to form H-dibaryons, which could give way to the formation of H-dibaryon matter at densities somewhere above $\sim 4\,n_0$ [89, 90, 91]. If formed in neutron stars, however, H-matter appears to unstable against compression which could trigger the conversion of neutron stars into hypothetical strange stars [90, 92, 93].

Another particle, referred to as exotic baryon, of potential relevance for neutron stars, could be the pentaquark, $\Theta^+([ud]^2\bar{s})$, with a predicted mass of 1540 MeV. The pentaquark, which carries baryon number one, is a hypothetical subatomic particle consisting of a group of four quarks and one anti-quark (compared to three quarks in normal baryons and two in mesons), bound by the strong color-spin correlation force (attraction between quarks in the color $\bar{\mathbf{3}}_c$ channel) that drives color superconductivity [94, 95]. The pentaquark decays according to $\Theta^+(1540) \rightarrow K^+[\bar{s}u] + n[udd]$ and thus has the same quantum numbers as the K^+n. The associated reaction in chemically equilibrated matter would imply $\mu^{\Theta^+} = \mu^{K^+} + \mu^n$.

3.4 Quark deconfinement

It has been suggested already many decades ago [96, 97, 98, 99, 100, 101, 102, 103] that the nucleons may melt under the enormous pressure that exists in the cores of neutron stars, creating a new state of matter know as quark matter. From simple geometrical considerations it follows that for a characteristic nucleon radius of $r_N \sim 1$ fm, nucleons may begin to touch each other in nuclear matter at densities around $(4\pi r_N^3/3)^{-1} \simeq 0.24\ \mathrm{fm}^{-3} = 1.5\,n_0$, which is less than twice the density of nuclear matter. This figure increases to $\sim 11\,n_0$ for a nucleon radius of $r_N = 0.5$ fm. One may thus speculate that the hadrons of neutron star matter begin to dissolve at densities somewhere between around

$2-10\,n_0$, giving way to unconfined quarks. Depending on rotational frequency and neutron star mass, densities greater than two to three times n_0 are easily reached in the cores of neutron stars so that the neutrons and protons in the cores of neutron stars may indeed be broken up into their quark constituents [6, 7, 11, 104]. More than that, since the mass of the strange quark is only $m_s \sim 150$ MeV, high-energetic up and down quarks will readily transform to strange quarks at about the same density at which up and down quark deconfinement sets in. Thus, if quark matter exists in the cores of neutron stars, it should be made of the three lightest quark flavors. A possible astrophysical signal of quark deconfinement in the cores of neutron stars was suggested in [105]. The remaining three quark flavors (charm, top, bottom) are way to massive to be created in neutron stars. For instance, the creation of charm quark requires a density greater than $10^{17}\,\mathrm{g/cm^3}$, which is around 100 times greater than the density reached in neutron stars. A stability analysis of stars with a charm quark population reveals that such objects are unstable against radial oscillations and, thus, can not exist stably in the universe [7, 11]. The same is true for ultra-compact stars with unconfined populations of top and bottom quarks, since the pulsation eigen-equations are of Sturm-Liouville type.

The phase transition from confined hadronic (H) matter to deconfined quark (Q) matter is characterized by the conservation of baryon charge and electric charge. The Gibbs condition for phase equilibrium then is that the two associated chemical potentials, μ^n and μ^e, and the pressure in the two phases be equal [6, 104],

$$P_{\rm H}(\mu^n, \mu^e, \{\chi\}, T) = P_{\rm Q}(\mu^n, \mu^e, T)\,, \tag{8}$$

The quantity $P_{\rm H}$ denotes the pressure of hadronic matter computed for a given hadronic Lagrangian $\mathcal{L}_{\rm M}(\{\chi\})$, where $\{\chi\}$ denotes the field variables and Fermi momenta that characterize a solution to the field equations of confined hadronic matter,

$$(i\gamma^\mu\partial_\mu - m_\chi)\psi_\chi(x) = \sum_{M=\sigma,\omega,\pi,\ldots} \Gamma_{M\chi} M(x)\,\psi_\chi(x)\,, \tag{9}$$

$$(\partial^\mu\partial_\mu + m_\sigma^2)\sigma(x) = \sum_{\chi=p,n,\Sigma,\ldots} \Gamma_{\sigma\chi}\,\bar\psi_\chi(x)\psi_\chi(x)\,, \tag{10}$$

plus additional equations for the other meson fields ($M = \omega, \pi, \rho, ...$). The pressure of quark matter, $P_{\rm Q}$, is obtainable from the bag model [106, 107]. The quark chemical potentials $\mu^u,\ \mu^d,\ \mu^s$ are related to the baryon and charge chemical potentials as

$$\mu^u = \frac{1}{3}\,\mu^n - \frac{2}{3}\,\mu^e\,, \qquad \mu^d = \mu^s = \frac{1}{3}\,\mu^n + \frac{1}{3}\,\mu^e\,. \tag{11}$$

Equation (8) is to be supplemented with the two global relations for conservation of baryon charge and electric charge within an unknown volume V containing A baryons. The first one is given by

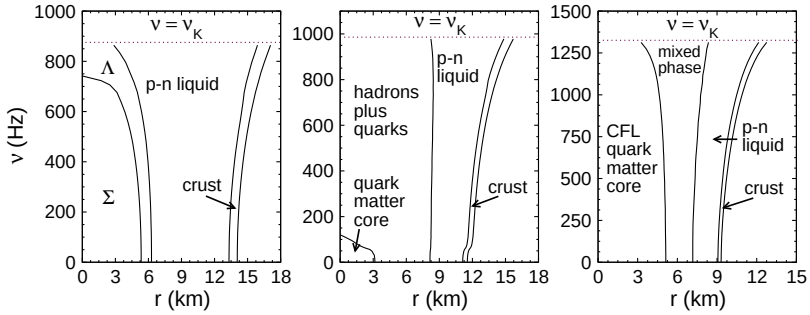

Fig. 7. Dependence of neutron star composition on spin frequency, ν, for three sample compositions (left: hyperon composition, middle: quark-hybrid composition, right: quark-hybrid composition with quark matter in the color-flavor locked (CFL) phase [108]). The non-rotating stellar mass in each case is $1.4\,M_\odot$. $\nu_{\rm K}$ denotes the Kepler (mass-shedding) frequency, which sets an absolute limit on stable rotation.

$$n \equiv \frac{A}{V} = (1-\eta)\, n_{\rm H}(\mu^n, \mu^e, T) + \eta\, n_{\rm Q}(\mu^n, \mu^e, T)\,, \tag{12}$$

where $\eta \equiv V_{\rm Q}/V$ denotes the volume proportion of quark matter, $V_{\rm Q}$, in the unknown volume V, and $n_{\rm H}$ and $n_{\rm Q}$ are the baryon number densities of hadronic matter and quark matter. Global neutrality of electric charge within the volume V can be written as

$$0 = \frac{Q}{V} = (1-\eta)\, q_{\rm H}(\mu^n, \mu^e, T) + \eta\, q_{\rm Q}(\mu^n, \mu^e, T) + q_{\rm L}\,, \tag{13}$$

with q_i the electric charge densities of hadrons, quarks, and leptons. For a given temperature, T, Eqs. (8) to (13) serve to determine the two independent chemical potentials and the volume V for a specified volume fraction η of the quark phase in equilibrium with the hadronic phase. After completion $V_{\rm Q}$ is obtained as $V_{\rm Q} = \eta V$. Because of Eqs. (8) through (13) the chemical potentials depend on the proportion η of the phases in equilibrium, and hence so also all properties that depend on them, i.e. the energy densities, baryon and charge densities of each phase, and the common pressure. For the mixed phase, the volume proportion of quark matter varies from $0 \le \eta \le 1$ and the energy density is the linear combination of the two phases [6, 104],

$$\epsilon = (1-\eta)\, \epsilon_{\rm H}(\mu^n, \mu^e, \{\chi\}, T) + \eta\, \epsilon_{\rm Q}(\mu^n, \mu^e, T)\,. \tag{14}$$

Hypothetical neutron star compositions computed along the lines described above are shown in Fig. 7. Possible astrophysical signals associated with quark deconfinement, the most striking of which being "backbending" of isolated pulsars, are discussed in [6, 7, 11, 109, 110].

3.5 Color-superconductivity

There has been much recent progress in our understanding of quark matter, culminating in the discovery that if quark matter exists it ought to be in a color superconducting state [22, 23, 24, 25]. This is made possible by the strong interaction among the quarks which is very attractive in some channels. Pairs of quarks are thus expected to form Cooper pairs very readily. Since pairs of quarks cannot be color-neutral, the resulting condensate will break the local color symmetry and form what is called a color superconductor. The phase diagram of such matter is expected to be very complex [22, 23]. The complexity is caused by the fact that quarks come in three different colors, different flavors, and different masses. Moreover, bulk matter is neutral with respect to both electric and color charge, and is in chemical equilibrium under the weak interaction processes that turn one quark flavor into another. To illustrate the condensation pattern briefly, we note the following pairing ansatz for the quark condensate [111],

$$\langle \psi^{\alpha}_{f_a} C\gamma_5 \psi^{\beta}_{f_b} \rangle \sim \Delta_1 \epsilon^{\alpha\beta 1}\epsilon_{f_a f_b 1} + \Delta_2 \epsilon^{\alpha\beta 2}\epsilon_{f_a f_b 2} + \Delta_3 \epsilon^{\alpha\beta 3}\epsilon_{f_a f_b 3}\,, \qquad (15)$$

where $\psi^{\alpha}_{f_a}$ is a quark of color $\alpha = (r, g, b)$ and flavor $f_a = (u, d, s)$. The condensate is a Lorentz scalar, antisymmetric in Dirac indices, antisymmetric in color, and thus antisymmetric in flavor. The gap parameters Δ_1, Δ_2 and Δ_3 describe d-s, u-s and u-d quark Cooper pairs, respectively. The following pairing schemes have emerged. At asymptotic densities ($m_s \to 0$ or $\mu \to \infty$) the ground state of QCD with a vanishing strange quark mass is the color-flavor locked (CFL) phase (color-flavor locked quark pairing), in which all three quark flavors participate symmetrically. The gaps associated with this phase are

$$\Delta_3 \simeq \Delta_2 = \Delta_1 = \Delta\,, \qquad (16)$$

and the quark condensates of the CFL phase are approximately of the form

$$\langle \psi^{\alpha}_{f_a} C\gamma_5 \psi^{\beta}_{f_b} \rangle \sim \Delta\, \epsilon^{\alpha\beta X}\epsilon_{f_a f_b X}\,, \qquad (17)$$

with color and flavor indices all running from 1 to 3. Since $\epsilon^{\alpha\beta X}\epsilon_{f_a f_b X} = \delta^{\alpha}_{f_a}\delta^{\beta}_{f_b} - \delta^{\alpha}_{f_b}\delta^{\beta}_{f_a}$ one sees that the condensate (17) involves Kronecker delta functions that link color and flavor indices. Hence the notion color-flavor locking. The CFL phase has been shown to be electrically neutral without any need for electrons for a significant range of chemical potentials and strange quark masses [112]. If the strange quark mass is heavy enough to be ignored, then up and down quarks may pair in the two-flavor superconducting (2SC) phase. Other possible condensation patterns are CFL-K^0 [113], CFL-K^+ and CFL-$\pi^{0,-}$ [114], gCFL (gapless CFL phase) [111], 1SC (single-flavor-pairing) [111, 115, 116], CSL (color-spin locked phase) [117], and the LOFF (crystalline pairing) [118, 119, 120] phase, depending on m_s, μ, and electric charge density. Calculations performed for massless up and down quarks and a very

heavy strange quark mass ($m_s \to \infty$) agree that the quarks prefer to pair in the two-flavor superconducting (2SC) phase where

$$\Delta_3 > 0\,, \quad \text{and} \quad \Delta_2 = \Delta_1 = 0\,. \tag{18}$$

In this case the pairing ansatz (15) reduces to

$$\langle \psi^{\alpha}_{f_a} C\gamma_5 \psi^{\beta}_{f_b} \rangle \propto \Delta\, \epsilon_{ab} \epsilon^{\alpha\beta 3}\,. \tag{19}$$

Here the resulting condensate picks a color direction (3 or blue in the example (19) above), and creates a gap Δ at the Fermi surfaces of quarks with the other two out of three colors (red and green). The gapless CFL phase (gCFL) may prevail over the CFL and 2SC phases at intermediate values of m_s^2/μ with gaps given obeying the relation $\Delta_3 > \Delta_2 > \Delta_1 > 0$. For chemical potentials that are of astrophysical interest, $\mu < 1000$ MeV, the gap is between 50 and 100 MeV. The order of magnitude of this result agrees with calculations based on phenomenological effective interactions [25, 121] as well as with perturbative calculations for $\mu > 10$ GeV [122]. We also note that superconductivity modifies the equation of state at the order of $(\Delta/\mu)^2$ [123, 124], which is even for such large gaps only a few percent of the bulk energy. Such small effects may be safely neglected in present determinations of models for the equation of state of quark-hybrid stars. There has been much recent work on how color superconductivity in neutron stars could affect their properties [22, 23, 118, 125, 126, 127]. These studies reveal that possible signatures include the cooling by neutrino emission, the pattern of the arrival times of supernova neutrinos, the evolution of neutron star magnetic fields, rotational stellar instabilities, and glitches in rotation frequencies.

4 Strange Quark Matter

It is most intriguing that for strange quark matter made of more than a few hundred up, down, and strange quarks, the energy of strange quark matter may be well below the energy of nuclear matter [15, 16, 17], $E/A = 930$ MeV, which gives rise to new and novel classes of strange matter objects, ranging from strangelets at the low baryon-number end to strange stars at the high baryon number end [7, 11, 18, 20, 128]. A simple estimate indicates that for strange quark matter $E/A = 4B\pi^2/\mu^3$, so that bag constants of $B = 57$ MeV/fm^3 (i.e. $B^{1/4} = 145$ MeV) and $B = 85$ MeV/fm^3 ($B^{1/4} = 160$ MeV) would place the energy per baryon of such matter at $E/A = 829$ MeV and 915 MeV, respectively, which correspond obviously to strange quark matter which is absolutely bound with respect to nuclear matter [20, 129].

4.1 Nuclear crust on strange stars

Strange quark matter is expected to be a color superconductor which, at extremely high densities, should be in the CFL phase [22, 23]. This phase is

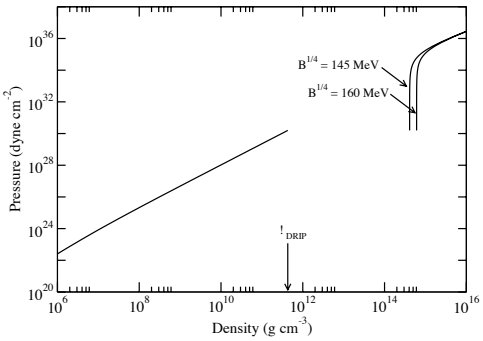

Fig. 8. Illustration of the eos of strange stars with nuclear crusts (from [130]).

rigorously electrically neutral with no electrons required [112]. For sufficiently large strange quark masses, however, the low density regime of strange quark matter is rather expected to form other condensation patterns (e.g. 2SC, CFL-K^0, CFL-K^+, CFL-$\pi^{0,-}$) in which electrons are present [22, 23]. The presence of electrons causes the formation of an electric dipole layer on the surface of strange matter, with huge electric fields on the order of 10^{19} V/cm, which enables strange quark matter stars to be enveloped in nuclear crusts made of ordinary atomic matter [18, 19, 63, 131].[4] The maximal possible density at the base of the crust (inner crust density) is determined by neutron drip, which occurs at about 4×10^{11} g/cm^3 or somewhat below [63]. The eos of such a system is shown in Fig. 8. Sequences of compact strange stars with and without (bare) nuclear crusts are shown in Fig. 3. Since the nuclear crust is gravitationally bound to the quark matter core, the mass-radius relationship of strange stars with crusts resembles the one of neutron stars and even that of white dwarfs [21]. Bare strange stars obey $M \propto R^3$ because the mass density of quark matter is almost constant inside strange stars.

4.2 Strange dwarfs

For many years only rather vague tests of the theoretical mass-radius relationship of white dwarfs were possible. Recently the quality and quantity of observational data on the mass-radius relation of white dwarfs has been re-analyzed and profoundly improved by the availability of Hipparcos parallax

[4] Depending on the surface tension of blobs of strange matter and screening effects, a heterogeneous crust comprised of blobs of strange quark matter embedded in an uniform electron background may exist in the surface region of strange stars [132]. This heterogeneous strange star surface would have a negligible electric field which would make the existence of an ordinary nuclear crust, which requires a very strong electric field, impossible.

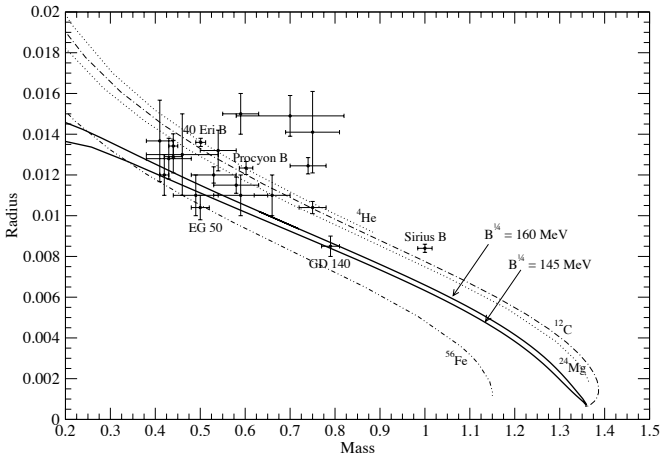

Fig. 9. Comparison of the theoretical mass-radius relationships of strange dwarfs (solid curves) and normal white dwarfs [130]. Radius and mass are in units of $R_\odot$ and $M_\odot$, respectively.

measurements of several white dwarfs [133]. In that work Hipparcos parallaxes were used to deduce luminosity radii for 10 white dwarfs in visual binaries of common proper-motion systems as well as 11 field white dwarfs. Complementary HST observations have been made to better determine the spectroscopy for Procyon B [134] and pulsation of G226-29 [135]. Procyon B at first appeared as a rather compact star which, however, was later confirmed to lie on the normal mass-radius relation of white dwarfs. Stars like Sirius B and 40 Erin B, fall nicely on the expected mass-radius relation too. Several other stars of this sample (e.g. GD 140, G156–64, EG 21, EG 50, G181–B5B, GD 279, WD2007–303, G238–44) however appear to be unusually compact and thus could be strange dwarf candidates [136]. The situation is graphically summarized in Fig. 9.

4.3 Surface properties of strange matter

The electrons surrounding strange quark matter are held to quark matter electrostatically. Since neither component, electrons and quark matter, is held in place gravitationally, the Eddington limit to the luminosity that a static surface may emit does not apply, and thus the object may have photon luminosities much greater than 10^{38} erg/s. It was shown by Usov [137] that this value may be exceeded by many orders of magnitude by the luminosity of e^+e^- pairs produced by the Coulomb barrier at the surface of a hot strange star.

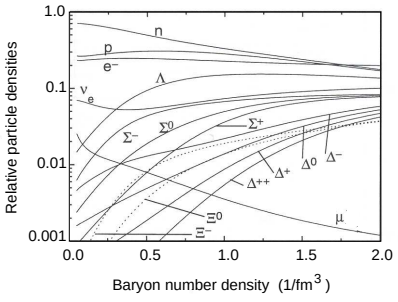

Fig. 10. Composition of hot (T = 40 MeV) proto-neutron star matter for $Y_L = 0.3$ [142].

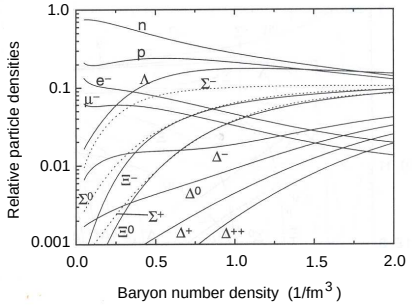

Fig. 11. Same as Fig. 10, but for standard neutron star matter [142].

For a surface temperature of $\sim 10^{11}$ K, the luminosity in the outflowing pair plasma was calculated to be as high as $\sim 3 \times 10^{51}$ erg/s. Such an effect may be a good observational signature of bare strange stars [137, 138, 139, 140]. If the strange star is enveloped by a nuclear crust however, which is gravitationally bound to the strange star, the surface made up of ordinary atomic matter would be subject to the Eddington limit. Hence the photon emissivity of such a strange star would be the same as for an ordinary neutron star. If quark matter at the stellar surface is in the CFL phase the process of e^+e^- pair creation at the stellar quark matter surface may be turned off, since cold CFL quark matter is electrically neutral so that no electrons are required and none are admitted inside CFL quark matter [112]. This may be different for the early stages of a hot CFL quark star [141].

5 Proto-Neutron Star Matter

Here we take a brief look at the composition of proto-neutron star matter. The composition is determined by the requirements of charge neutrality and equilibrium under the weak processes, $B_1 \to B_2 + l + \bar{\nu}_l$ and $B_2 + l \to B_1 + \nu_l$, where B_1 and B_2 are baryons, and l is a lepton, either an electron or a muon. For standard neutron star matter, where the neutrinos have left the system, these two requirements imply that $Q = \sum_i q_i n_{B_i} + \sum_{l=e,\mu} q_l n_l = 0$ (electric charge neutrality) and $\mu_{B_i} = b_i \mu_n - q_i \mu_l$ (chemical equilibrium), where $q_{i/l}$ denotes the electric charge density of a given particle, and n_{B_i} (n_l) is the baryon (lepton) number density. The subscript i runs over all the baryons considered. The symbol μ_{B_i} refers to the chemical potential of baryon i, b_i is the particle's baryon number, and q_i is its charge. The chemical potential of the neutron is denoted by μ_n. When the neutrinos are trapped, as it is the case for proto-neutron star matter, the chemical equilibrium condition is

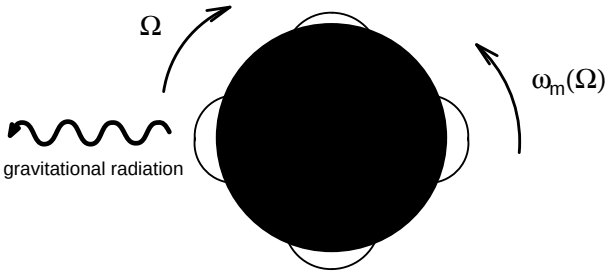

Fig. 12. Representation of an $m = 4$ perturbation of a rotating neutron star. Ω denotes the star's rotational frequency, ω_m is the frequency of the counter-rotating perturbation [7].

altered to $\mu_{B_i} = b_i\mu_n - q_i(\mu_l - \mu_{\nu_l})$ and $\mu_e - \mu_{\nu_e} = \mu_\mu - \mu_{\nu_\mu}$, where μ_{ν_l} is the chemical potential of the neutrino ν_l. In proto-neutron star matter, the electron lepton number $Y_L = (n_e + n_{\nu_e})/n_B$ is initially fixed at a value of around $Y_{L_e} = Y_e + Y_{\nu_e} \simeq 0.3 - 0.4$ as suggested by gravitational collapse calculations of massive stars. Also, because no muons are present when neutrinos are trapped, the constraint $Y_{L_\mu} = Y_\mu + Y_{\nu_m u} = 0$ can be imposed. Figures 10 and 11 show sample compositions of proto-neutron star matter and standard neutron star matter (no neutrinos) computed for the relativistic mean-field approximation. The presence of the Δ particle in (proto) neutron star matter at finite temperature is striking. This particle is generally absent in cold neutron star matter treated in the relativistic mean-field approximation [6, 7, 143].

6 Rotational Instabilities

An absolute limit on rapid rotation is set by the onset of mass shedding from the equator of a rotating star. However, rotational instabilities in rotating stars, known as gravitational radiation driven instabilities, set a more stringent limit on rapid stellar rotation than mass shedding. These instabilities originate from counter-rotating surface vibrational modes which at sufficiently high rotational star frequencies are dragged forward, as schematically illustrated in Fig. 12. In this case gravitational radiation, which inevitably accompanies the aspherical transport of matter, does not damp the instability modes but rather drives them. Viscosity plays the important role of damping these instabilities at a sufficiently reduced rotational frequency such that the viscous damping rate and power in gravity waves are comparable. The most critical instability modes that are driven unstable by gravitational radiation are f-modes [7, 144] and r-modes [145, 146]. Figure 13 shows the stable neutron star frequencies if only f-modes were operative in neutron star. One sees that hot as well as cold neutron stars can rotate at frequencies close to mass shedding, because of the large contributions of shear and bulk viscosity, respectively, for this temperature regime. The more recently discovered r-mode instability [145,

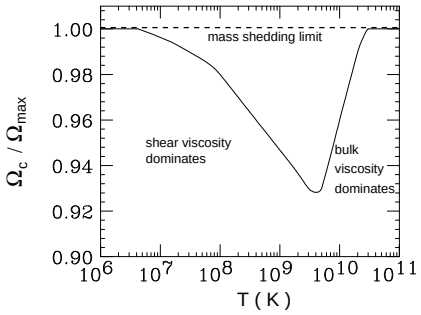

Fig. 13. Gravitational radiation driven f-mode instability suppressed by shear and bulk viscosity. (Fig. from [7].)

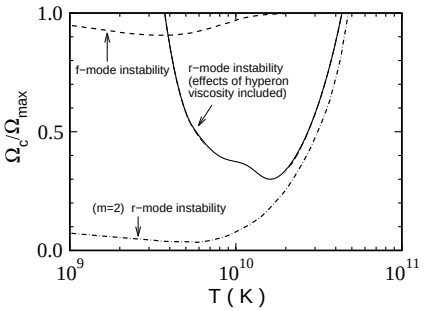

Fig. 14. Comparison of f-mode instability with r-mode instability. (Data from Refs. [144, 147].)

148] may change the picture completely, as can be seen from Fig. 14. These modes are driven unstable by gravitational radiation over a considerably wider range of angular velocities than the f-modes (cf. dashed curve labeled ($m = 2$) r-mode instability). In stars with cores cooler than $\sim 10^9$ K, on the other hand, the r-mode instability may be completely suppressed by the viscosity originating from the presence of hyperons in neutron star matter, so that stable rotation would be limited by the f-mode instability again [147].

Figures 15 and 16 are the counterparts to Figs. 13 and 14 but calculated for strange stars made of CFL and 2SC quark matter, respectively [149, 150]. The r-mode instability seems to rule out that pulsars are CFL strange stars, if the characteristic time scale for viscous damping of r-modes are exponentially increased by factors of $\sim \Delta/T$ as calculated in [149]. An energy gap as small as $\Delta = 1$ MeV was assumed. For much larger gaps of $\Delta \sim 100$ MeV, as expected for color superconducting quark matter (see section 3.5), the entire diagram would be r-mode unstable. The full curve in Fig. 15 is calculated for a strange quark mass of $m_s = 200$ MeV, the dotted curve for $m_s = 100$ MeV. The box marks the positions of most low mass X-ray binaries (LMXBs) [151], and the crosses denote the most rapidly rotating millisecond pulsars known. All strange stars above the curves would spin down on a time scale of hours due to the r-mode instability, in complete contradiction to the observation of millisecond pulsars and LMXBs, which would rule out CFL quark matter in strange stars (see, however, [152]). Figure 16 shows the critical rotation frequencies of quark stars as a function of internal stellar temperature for 2SC quark stars. For such quark stars the situation is less conclusive. Rapid spin-down, driven by the r-mode gravitational radiation instability, would happen for stars above the curves.

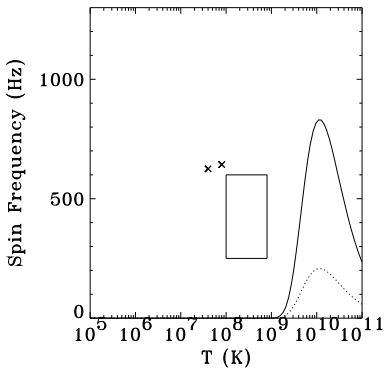

Fig. 15. Critical rotation frequencies versus stellar temperature for CFL strange stars [150].

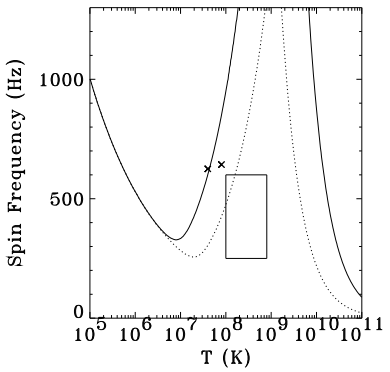

Fig. 16. Same as Fig. 15, but for 2SC quark stars [150].

7 Net Electric Fields and Compact Star Structure

Here we consider the possibility that the electric charge density inside compact stars (neutron stars, strange stars) is not identically zero. This may be the case, for example, for compact stars accreting ionized hydrogen. Another example are strange quark stars. They could have electric charge distributions on their surfaces that generate electric fields on the order of 10^{18} V/cm [7, 11, 18, 131] for ordinary quark matter, and 10^{19} V/cm [153] if quark matter is a color-superconductor. Although the electric field on strange stars exists only in a very narrow region of space, it is interesting to study the effects of such ultra-high electric fields on the structure of the star.

It has already been shown that the energy densities of ultra-high electric fields can substantially alter the structure (mass–radius relationship) of compact stars [154], depending on the strength of the electric field. In contrast to electrically uncharged stars, the energy-momentum tensor of charged stars has two key contributions, the usual matter-energy term plus the energy density term that originates from the electric field. The latter plays a dual role for compact star physics. Firstly, it acts as an additional source of gravity and, secondly, it introduces Coulomb interactions inside the star. Both features can alter the properties of compact stars significantly, as we shall demonstrate below.

We will restrict ourselves to spherically symmetric compact stars. The metric of such objects is given by

$$ds^2 = e^{\nu(r)}c^2dt^2 - e^{\lambda(r)}dr^2 - r^2(d\theta^2 + \sin^2\theta d\phi^2)\,. \qquad (20)$$

The energy-momentum tensor consists of the usual perfect fluid term supplemented with the electromagnetic energy-momentum tensor,

$$T_\kappa{}^\mu = (p+\rho c^2)u_\kappa u^\mu + p\delta_\kappa{}^\mu + \frac{1}{4\pi}\left[F^{\mu l}F_{\kappa l} + \frac{1}{4\pi}\delta_\kappa{}^\mu F_{kl}F^{kl}\right], \qquad (21)$$

where u^μ is the fluid's four-velocity, p and $\rho c^2 \equiv \epsilon$ are the pressure and energy density, respectively, and $F^{\mu\kappa}$ satisfies the covariant Maxwell equation,

$$[(-g)^{1/2}F^{\kappa\mu}]_{,\mu} = 4\pi J^\kappa (-g)^{1/2}. \qquad (22)$$

The quantity J^κ denotes the four-current which represents the electromagnetic sources in the star. For a static spherically symmetric system, the only non-zero component of the four-current is J^1, which implies that the only non-vanishing component of $F^{\kappa\mu}$ is F^{01}. We therefore obtain from Eq. (22)

$$F^{01}(r) = E(r) = r^{-2}\, e^{-(\nu+\lambda)/2}\int_0^r 4\pi j^0 e^{(\nu+\lambda)/2}dr\,, \qquad (23)$$

which is nothing other than the electric field. This relation can be identified as the relativistic version of Gauss' law. In addition we see that the electric charge of the system is given by

$$Q(r) = \int_0^r 4\pi j^0 e^{(\nu+\lambda)/2}dr\,. \qquad (24)$$

With the aid of Eq. (24) the energy-momentum tensor of the system can be written as

$$T_\kappa{}^\mu = \begin{pmatrix} -\left(\epsilon + \frac{Q^2(r)}{8\pi r^4}\right) & 0 & 0 & 0 \\ 0 & p - \frac{Q^2(r)}{8\pi r^4} & 0 & 0 \\ 0 & 0 & p + \frac{Q^2(r)}{8\pi r^4} & 0 \\ 0 & 0 & 0 & p + \frac{Q^2(r)}{8\pi r^4} \end{pmatrix}. \qquad (25)$$

Using the energy-momentum tensor (25), Einstein's field equation leads to

$$e^{-\lambda}\left(-\frac{1}{r^2} + \frac{1}{r}\frac{d\lambda}{dr}\right) + \frac{1}{r^2} = \frac{8\pi G}{c^4}\left(p - \frac{Q^2(r)}{8\pi r^4}\right), \qquad (26)$$

$$e^{-\lambda}\left(\frac{1}{r}\frac{d\kappa}{dr} + \frac{1}{r^2}\right) - \frac{1}{r^2} = -\frac{8\pi G}{c^4}\left(\epsilon + \frac{Q^2(r)}{8\pi r^4}\right). \qquad (27)$$

At this point we define the radial component of the metric g^{11}, in analogy to the exterior solution of Reissner-Nordström, as [155]

$$e^{-\lambda}(r) = 1 - \frac{Gm(r)}{rc^2} + \frac{GQ^2(r)}{r^2c^4}\,. \qquad (28)$$

From equations (26), (27) and (28), we derive an expression for $m(r)$, which is interpreted as the total mass of the star at a radial distance r. This expression reads

$$\frac{dm(r)}{dr} = \frac{4\pi r^2}{c^2}\epsilon + \frac{Q(r)}{c^2 r}\frac{dQ(r)}{dr}\,, \tag{29}$$

which reveals that, in addition to the standard term originating from the eos of the stellar fluid, the electric field energy contributes to the star's total mass too. Next, we impose the vanishing of the divergence of the energy-momentum tensor, $T^{\mu}{}_{\kappa;\mu} = 0$, which leads to the Tolman-Oppenheimer-Volkoff (TOV) equation of electrically charged stars,

$$\frac{dp}{dr} = -\frac{2G\left[m(r) + \frac{4\pi r^3}{c^2}\left(p - \frac{Q^2(r)}{4\pi r^4 c^2}\right)\right]}{c^2 r^2\left(1 - \frac{2Gm(r)}{c^2 r} + \frac{GQ^2(r)}{r^2 c^4}\right)}(p+\epsilon) + \frac{Q(r)}{4\pi r^4}\frac{dQ(r)}{dr}\,. \tag{30}$$

Summarizing the relevant stellar structure equations, we end up with the following set of equations:

$$\frac{d\lambda}{dr} = \frac{8\pi G}{c^4}\left(\epsilon + \frac{Q^2(r)}{8\pi r^4}\right) r e^{\lambda} - \left(\frac{e^{-\lambda} - 1}{r}\right)\,, \tag{31}$$

$$\frac{d\nu}{dr} = \frac{2G\left[m(r) + \frac{4\pi r^3}{c^2}\left(p - \frac{Q^2(r)}{4\pi r^4 c^2}\right)\right]}{c^2 r^2\left(1 - \frac{2Gm(r)}{c^2 r} + \frac{GQ^2(r)}{r^2 c^4}\right)}\,. \tag{32}$$

$$\frac{dm(r)}{dr} = \frac{4\pi r^2}{c^2}\epsilon + \frac{Q(r)}{c^2 r}\frac{dQ(r)}{dr}, \tag{33}$$

$$\frac{dQ(r)}{dr} = 4\pi r^2 j^0 e^{-(\nu+\lambda)/2}\,. \tag{34}$$

$$\frac{dp}{dr} = -\frac{2G\left[m(r) + \frac{4\pi r^3}{c^2}\left(p - \frac{Q^2(r)}{4\pi r^4 c^2}\right)\right]}{c^2 r^2\left(1 - \frac{2Gm(r)}{c^2 r} + \frac{GQ^2(r)}{r^2 c^4}\right)}(p+\epsilon) + \frac{Q(r)}{4\pi r^4}\frac{dQ(r)}{dr}\,. \tag{35}$$

Equations (31) and (32) arise from Einstein's field equation, Eq. (33) is the mass continuity equation, Eq. (34) comes from the Maxwell equations, and Eq. (35) is the TOV equation. This system of coupled differential equations is subject to the following boundary conditions

$$p(0) = p_c\,, \quad e^{\lambda} = 0\,, Q(0) = 0\,, \quad m(0) = 0\,. \tag{36}$$

In addition to these conditions, one needs to specify the star's central density (or, equivalently, the central pressure) for a given equation of state and a given electric charge distribution. This will be discussed in more details in the next sections.

As already mentioned at the beginning of this section, strange stars may be expected to carry huge electric fields on their surfaces [7, 11, 18, 131, 153]. We want to study the effects of such fields on the overall structure of strange

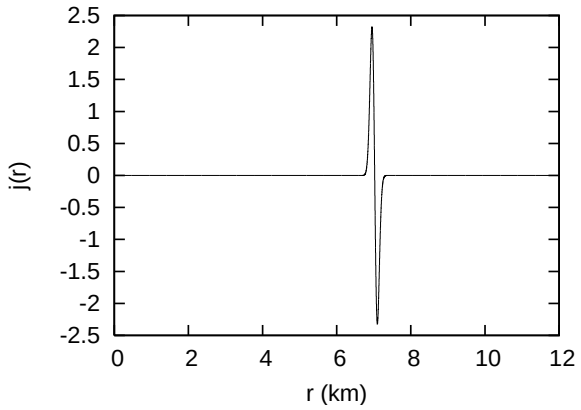

Fig. 17. Displacement of electric charges on the surface of a strange star. The mathematical form is obtained by superimposing two Gaussian functions.

stars. To this aim, we model the charge distribution by superimposing two Gaussian functions. The first Gaussian is chosen to be positive, representing the accumulation of a net positive charge. The second Gaussian, slightly displaced from the first one, is chosen negative to represent the accumulation of a net negative charge. Mathematically, we thus have

$$j(r) = \frac{\sigma}{b\sqrt{\pi}} \left(e^{-\left(\frac{r-r_1}{b}\right)^2} - e^{-\left(\frac{r-r_2}{b}\right)^2} \right), \tag{37}$$

where σ is a constant that controls the magnitude of the Gaussians and b the widths of the Gaussians. The graphical illustration of Eq. (37) is shown in Fig. 17. To obtain a noticeable impact of the electric field on the structure of strange stars, one needs to have Gaussians with a width of at least around 0.05 km. For such widths we find the mass–radius relationships shown in Fig. 18. The deviations from the mass-radius relationships of uncharged strange stars are found to increase with mass, and are largest for the maximum-mass star of each stellar sequence.

The radial distribution of the electric charge over the surface of a strange star is particularly interesting. The reason being the occurrence of the metric functions in Eq. (24), which defines the star's total net charge. Since the metric functions are not symmetric in the radial distance, the charge distribution is rendered asymmetric and stars that are strictly electrically charge neutral in flat space-time become electrically charged and thus possess non-zero electric fields. Figures 19 shows the electric field at the surface of strange stars. Figure 20 shows the net electric charge at the surface of strange stars. Both plots account for the general relativistic charge separation effect.

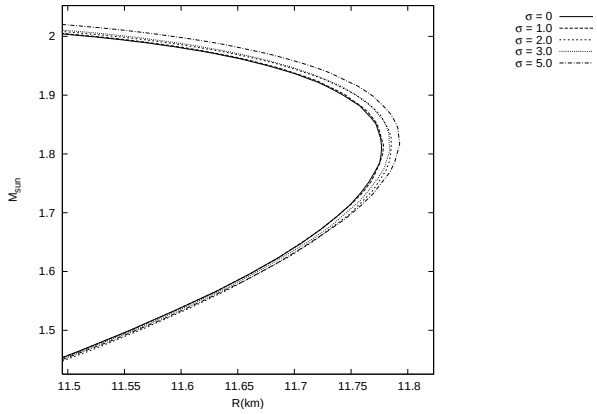

Fig. 18. Mass–radius relationships of electrically charged strange stars.

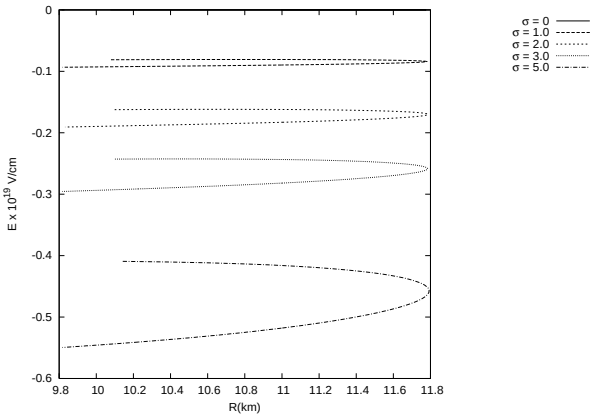

Fig. 19. Electric fields at the surface of strange stars.

8 Conclusions and Outlook

It is often stressed that there has never been a more exciting time in the overlapping areas of nuclear physics, particle physics and relativistic astrophysics than today. This comes at a time where new orbiting observatories such as the Hubble Space Telescope (HST), Rossi X-ray Timing Explorer, Chandra X-ray satellite, and the X-ray Multi Mirror Mission (XMM Newton) have extended our vision tremendously, allowing us to observe compact star phenomena with an unprecedented clarity and angular resolution that previously were only imagined. On the Earth, radio telescopes like Arecibo, Green Bank, Parkes, VLA, and instruments using adaptive optics and other revolutionary techniques have exceeded previous expectations of what can be accomplished from the ground. Finally, the gravitational wave detectors

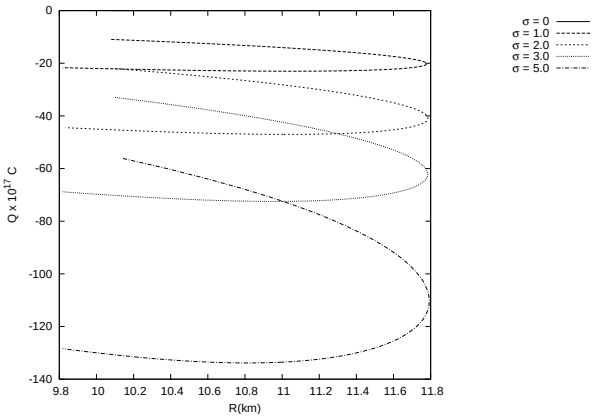

Fig. 20. Electric charge on strange quark stars.

LIGO, LISA, VIRGO, and Geo-600 are opening up a window for the detection of gravitational waves emitted from compact stellar objects such as neutron stars and black holes. This unprecedented situation is providing us with key information on neutron stars, which contain cold and ultra-dense baryonic matter permanently in their cores. As discussed in this paper, a key role in neutron star physics is played by strangeness. It alters the masses, radii, moment of inertia, frame dragging of local inertial frames, cooling behavior, and surface composition of neutron stars. Other important observables influenced by strangeness may be the spin evolution of isolated neutron stars and neutron stars in low-mass x-ray binaries. All told, these observables play a key role for the exploration of the phase diagram of dense nuclear matter at high baryon number density but low temperature [184], which is not accessible to relativistic heavy ion collision experiments.

Obviously, our understanding of neutron stars has changed dramatically since their first discovery some 40 years ago. In what follows, I briefly summarize what we have learned about the internal structure of these fascinating object since their discovery. I will address some of the most important open questions regarding the composition of neutron star matter and its associated equation of state, and will mention new tools, telescopes, observations, and calculations that are needed to answer these questions:

- There is no clear picture yet as to what kind of matter exists in the cores of neutron stars. They may contain significant hyperon populations, boson condensates, a mixed phase of quarks and hadrons, and/or pure quark matter made of unconfined up, down, and strange quarks.
- Pure neutron matter constitutes an excited state relative to many-baryon matter and, therefore, will quickly transform via weak reactions to such matter.

Table 1. Past, present, and future search experiments for strange quark matter [11].

Experiment	References
Cosmic ray searches for strange nuggets:	
AMS-02[a]	[156, 157]
CRASH[b]	[158, 159, 160]
ECCO[c]	[161]
HADRON	[162]
IMB[d]	[163]
JACEE[e]	[164, 165]
MACRO[f]	[166, 167, 168, 169]
Search for strangelets in terrestrial matter:	[170]
Tracks in ancient mica	[171, 172]
Rutherford backscattering	[173, 174]
Search for strangelets at accelerators:	
Strangelet searches E858, E864, E878, E882-B, E896-A, E886	[175, 176, 177]
H-dibaryon search	[178, 179]
Pb+Pb collisions	[180, 181, 182, 183]

[a] AMS: Alpha Magnetic Spectrometer (scheduled for 2005-2008).
[b] CRASH: Cosmic Ray And Strange Hadronic matter.
[c] ECCO: Extremely-heavy Cosmic-ray Composition Observer.
[d] IMB: Irvine Michigan Brookhaven proton-decay detector (1980-1991).
[e] JACEE: Japanese-American Cooperative Emulsion Chamber Experiment.
[f] MACRO: Monopole, Astrophysics and Cosmic Ray Observatory (1989-2000).

- Neutron stars made up of pure, interacting neutron matter cannot rotate as rapidly as the very recently discovered pulsars PSR J1748-2446ad, which spins at 716 Hz. The equation of state of such matter, therfore, imposes an upper bound on the equation of state of neutron star matter that is tighter than the usual $P = \epsilon$ constraint (see Fig. 2).
- Charm quarks do not play a role for neutron star physics, since they become populated at densities which are around 100 times greater than the densities encountered in the cores of neutron stars. While hydrostatically stable, "charm" stars are unstable against radial oscillations and, thus, cannot exist stably in the universe [131].
- Multi-quark states like the H-particle appear to make neutron stars unstable.
- Significant populations of Δ's are predicted by relativistic Brueckner-Hartree-Fock calculations, but not by standard mean-field calculations which do not account for dynamical correlations among baryons computed from the relativistic T-matrix equation.
- The finite temperatures of proto neutron stars favors the population of Δ's already at the mean-field level.

- The r-modes are of key interest for several reasons: 1. they may explain why young neutron stars spin slowly, 2. why rapidly accreting neutron stars (LMXB) spin slowly and within a narrow band, and 3. they may produce gravitational waves detectable by LIGO. Knowing the bulk viscosity originating from processes like $n+n- > p^+ + \Sigma^-$ and the superfluid critical temperature of Σ^-, both are poorly understood at present, will be key.
- The loss of pressure resulting from the appearance of additional hadronic degrees of freedom at high densities reduces the (maximum) mass of neutron stars. This feature may serve as a key criteria to distinguish between, and eliminate certain, classes of equations of state [6, 7, 185].
- Heavy neutron stars, with masses of around two solar masses, do not automatically rule out the presence of hyperons or quarks in the cores of neutron stars [186].
- Depending on the densities reached in the cores of neutron stars, both Schroedinger-based models as well as relativistic field-theoretical models may be applicable to neutron star studies.
- The density dependence of the coupling constants of particles in ultra-dense neutron star matter needs be taken into account in stellar structure calculations. Density dependent relativistic field theories are being developed which account for this feature..
- The models used to study the quark-hadron phase transition in the cores of neutron stars are extremely phenomenological and require considerable improvements.
- If quark matter exists in the cores of neutron stars, it will be a color superconductor whose complex condensation pattern is likely to change with density inside the star. The exploration of the numerous astrophysical facets of (color superconducting) quark matter is therefore of uppermost importance. What are the signatures of color superconducting quark matter in neutron stars? So far it has mostly been demonstrated that color superconductivity is compatible with observed neutron star properties.
- A two-step quark-hadron phase transition (1. from nuclear matter to regular quark matter, 2. from regular quark matter to color superconducting quark matter) may explain long quiescent gamma-ray bursts due to the two phase transitions involved.
- Are there isolated pulsar that are spinning up? Such a (backbending) phenomenon could be caused by a strong first-order-like quark-hadron phase transitions in the core of a neutron star [105, 187, 188].
- Was the mass of the neutron star created in SN 1987A around $1.5 M_\odot$? And did SN 1987A go into a black hole or not? If the answer to both questions were yes, a serious conflict with the observation of heavy neutron stars would arise. On the other hand, it could also indicate the existence generically different classes of "neutron" stars with very different maximum masses.

- Sources known to increase the masses of neutron stars are differential rotation, magnetic fields, and electric fields. Some of these sources are more effective (and plausible) than others though.
- Nuclear processes in non-equilibrium nuclear crusts (e.g. pycnonuclear reactions) and/or cores (heating caused by changes in the composition) of neutron stars can alter the thermal evolution of such stars significantly. We are just beginning to study these processes in greater detail.
- What is the shell structure for very neutron rich nuclei in the crusts of neutron stars?
- Do N=50 and N=82 remain magic numbers? Such questions will be addressed at GSI (Darmstadt) and RIKEN.
- Are there pulsars that rotate below one millisecond? Such objects may be composed of absolutely stable strange quark matter instead of purely gravitationally bound hadronic matter. Experimental physicists have searched unsuccessfully for stable or quasistable strange matter systems over the past two decades. These searches fall in three main categories: (a) searches for strange matter (strange nuggets or strangelets) in cosmic rays, (b) searches for strange matter in samples of ordinary matter, and (c) attempts to produce strange matter at accelerators. An overview of these search experiments is given in table 1.
- Strange stars may be enveloped in a crust. There is a critical surface tension below which the quark star surfaces will fragment into a crystalline crust made of charged strangelets immersed in an electron gas [128, 132]
- If bare, the quark star surface will have peculiar properties which distinguishes a quark star from a neutron star [137, 138, 189, 190].
- A very high-luminosity flare took place in the Large Magellanic Cloud (LMC), some 55 kpc away, on 5 March 1979. Another giant flare was observed on 27 August 1998 from SGR 1900+14. The inferred peak luminosities for both events is $\sim 10^7$ times the Eddington limit for a solar mass object, and the rise time is very much smaller than the time needed to drop $\sim 10^{25}$ g (about $10^{-8} M_\odot$) of normal material onto a neutron star. Alcock *et al.* [18] suggested a detailed model for the 5 March 1979 event burst which involves the particular properties of strange matter (see also [190, 191]). The model assumes that a lump of strange matter of $\sim 10^{-8}\, M_\odot$ fell onto a rotating strange star. Since the lump is entirely made up of self-bound high-density matter, there would be only little tidal distortion of the lump, and so the duration of the impact can be very short, around $\sim 10^{-6}$ s, which would explain the observed rapid onset of the gamma ray flash. The light curves expected for such giant bursts [137, 138, 139, 140] should posses characteristic features that are well within the capabilities of ESA's INTErnational Gamma-Ray Astrophysics Laboratory (INTEGRAL [192]) launched by the European Space Agency in October of 2002.

Acknowledgments

This material is based upon work supported by the National Science Foundation under Grant No. 0457329, and by the Research Corporation.

References

1. J. W. T. Hessels, S. M. Ransom, I. H. Stairs, P. C. C. Freire, V. M. Kaspi, and F. Camilo, Science **311** (2006) 1901.
2. D. C. Backer, S. R. Kulkarni, C. Heiles, M. M. Davis, and W. M. Goss, Nature **300** (1982) 615.
3. A. S. Fruchter, D. R. Stinebring, and J. H. Taylor, Nature **334** (1988) 237.
4. P. Kaaret *et al.*, Astrophys. J. **657** (2007) L97.
5. L. Villain, EAS Publ. Ser. 21 (2006) 335.
6. N. K. Glendenning, *Compact Stars, Nuclear Physics, Particle Physics, and General Relativity*, 2nd ed. (Springer-Verlag, New York, 2000).
7. F. Weber, *Pulsars as Astrophysical Laboratories for Nuclear and Particle Physics*, High Energy Physics, Cosmology and Gravitation Series (IOP Publishing, Bristol, Great Britain, 1999).
8. H. Heiselberg and V. Pandharipande, Ann. Rev. Nucl. Part. Sci. **50** (2000) 481.
9. J. M. Lattimer and M. Prakash, Astrophys. J. **550** (2001) 426.
10. *Physics of Neutron Star Interiors*, ed. by D. Blaschke, N. K. Glendenning, and A. Sedrakian, Lecture Notes in Physics **578** (Spring-Verlag, Berlin, 2001).
11. F. Weber, Prog. Part. Nucl. Phys. **54** (2005) 193, (`astro-ph/0407155`).
12. A. Sedrakian, Prog. Part. Nucl. Phys. **58** (2007) 168.
13. D. Page and S. Reddy, Ann. Rev. Nucl. Part. Sci. **56** (2006) 327.
14. D. Blaschke and H. Grigorian, *Unmasking neutron star interiors using cooling simulations*, to appear in Prog. Part. Nucl. Phys., (`arXiv:astro-ph/0612092`).
15. A. R. Bodmer, Phys. Rev. D **4** (1971) 1601.
16. E. Witten, Phys. Rev. D **30** (1984) 272.
17. H. Terazawa, INS-Report-338 (INS, Univ. of Tokyo, 1979); J. Phys. Soc. Japan, **58** (1989) 3555; **58** (1989) 4388; **59** (1990) 1199.
18. C. Alcock, E. Farhi, and A. V. Olinto, Astrophys. J. **310** (1986) 261.
19. C. Alcock and A. V. Olinto, Ann. Rev. Nucl. Part. Sci. **38** (1988) 161.
20. J. Madsen, Lecture Notes in Physics **516** (1999) 162.
21. N. K. Glendenning, Ch. Kettner, and F. Weber, Phys. Rev. Lett. **74** (1995) 3519.
22. K. Rajagopal and F. Wilczek, *The Condensed Matter Physics of QCD*, At the Frontier of Particle Physics / Handbook of QCD, ed. M. Shifman, (World Scientific) (2001).
23. M. Alford, Ann. Rev. Nucl. Part. Sci. **51** (2001) 131.
24. M. Alford, K. Rajagopal, and F. Wilczek, Phys. Lett. **422B** (1998) 247.
25. R. Rapp, T. Schäfer, E. V. Shuryak, and M. Velkovsky, Phys. Rev. Lett. **81** (1998) 53; Ann. Phys. **280** (2000) 35.
26. J. R. Oppenheimer and G. M. Volkoff, Phys. Rev. **55** (1939) 374.
27. R. C. Tolman, Phys. Rev. **55** (1939) 364.

28. J. H. Taylor and J. M. Weisberg, Astrophys. J. **345** (1989) 434.
29. S. E. Thorsett and D. Chakrabarty, Astrophys. J. **512** (1999) 288.
30. D. J. Nice, E. M. Splaver, I. H. Stairs, O. Loehmer, A. Jessner, M. Kramer, and J. M. Cordes, *A 2.1 solar mass pulsar measured by relativistic orbital decay*, (`astro-ph/0508050`).
31. D. Barret, J.-F. Olive, and M. C. Miller, *The coherence of kHz quasi-periodic oscillations in the X-rays from accreting neutron stars*, (`astro-ph/0605486`).
32. O. Barziv, L. Kaper, M. H. van Kerkwijk, J. H. Telting, and J. van Paradijs, Astron. & Astrophys. **377** (2001) 925.
33. J. Casares, P. A. Charles, and E. Kuulkers, Astrophys. J. **493** (1998) L39.
34. J. A. Orosz and E. Kuulkers, Mon. Not. R. Astron. Soc. **305** (1999) 132.
35. J. S. Clark, S. P. Goodwin, P. A. Crowther, L. Kaper, M. Fairbairn, N. Langer, and C. Brocksopp, Astron. & Astrophys. **392** (2002) 909.
36. T. Shahbaz, J. Casares, C. A. Watson, P. A. Charles, R. I. Hynes, S. C. Shih, and D. Steeghs, Astrophys. J. **616** (2004) L123.
37. C. E. Rhoades and R. Ruffini, Phys. Rev. Lett. **32** (1974) 324.
38. A. G. Sabbadini and J. B. Hartle, Ann. Phys. (N.Y.) **104** (1977) 95.
39. J. B. Hartle, Phys. Rep. **46** (1978) 201.
40. G. E. Brown and H. A. Bethe, Astrophys. J. **423** (1994) 659.
41. W. D. Myers and W. J. Swiatecki, Nucl. Phys. **A601** (1996) 141.
42. K. Strobel, F. Weber, M. K. Weigel, and Ch. Schaab, Int. J. Mod. Phys. E **6**, No. 4 (1997) 669.
43. V. R. Pandharipande and R. B. Wiringa, Rev. Mod. Phys. **51** (1979) 821.
44. R. B. Wiringa, V. Fiks, and A. Fabrocini, Phys. Rev. C **38** (1988) 1010.
45. A. Akmal, V. R. Pandharipande, and D. G. Ravenhall, Phys. Rev. C **58** (1998) 1804.
46. M. Baldo, G. F. Burgio, and H. J. Schulze, Phys. Rev. C **61** (2000) 055801.
47. M. Baldo and F. Burgio, Lect. Notes Phys. **578** (2001) 1.
48. G. F. Burgio, M. Baldo, H.-J. Schulze, and P. K. Sahu, Phys. Rev. C **66** (2002) 025802.
49. H. Lenske and C. Fuchs, Phys. Lett. **345B** (1995) 355.
50. C. Fuchs, H. Lenske, and H. H. Wolter, Phys. Rev. C **52** (1995) 3043.
51. S. Typel and H. H. Wolter, Nucl. Phys. **A656** (1999) 331.
52. F. Hofmann, C. M. Keil, and H. Lenske, Phys. Rev. C **64** (2001) 034314.
53. T. Nikšić, D. Vretenar, P.Finelli and P. Ring, Phys. Rev. C **66** (2002) 024306.
54. S. F. Ban, J. Li, S. Q. Zhang, H. Y. Jia, and J. P. Sang, and J. Meng, Phys. Rev. C **69** (2004) 045805.
55. M. Buballa, Phys. Rept. **407** (2005) 205.
56. D. Blaschke, S. Fredriksson, H. Grigorian, A. M. Öztas and F. Sandin, Phys. Rev. D **72** (2005) 065020.
57. S. B. Ruster, V. Werth, M. Buballa, I. A. Shovkovy, and D. H. Rischke, Phys. Rev. D **72** (2005) 034004.
58. H. Abuki and T. Kunihiro, Nucl. Phys. A **768** (2006) 118.
59. S. Lawley, W. Bentz, and A. W. Thomas, J. Phys. G: Nucl. Part. Phys. **32** (2006) 667.
60. S. Lawley, W. Bentz, and A. W. Thomas, Phys. Lett. **B632** (2006) 495.
61. P. Wang, S. Lawley, D. B. Leinweber, A. W. Thomas, and A. G. Williams, Phys. Rev. C **72** (2005) 045801.
62. N. K. Glendenning and F. Weber, Astrophys. J. **400** (1992) 647.

63. M. Stejner and J. Madsen, Phys. Rev. D **72** (2005) 123005.
64. N. K. Glendenning, Astrophys. J. **293** (1985) 470.
65. H. Huber, F. Weber, M. K. Weigel, and Ch. Schaab, Int. J. Mod. Phys. E **7**, No. 3 (1998) 301.
66. M. Prakash, I. Bombaci, M. Prakash, P. J. Ellis, J. M. Lattimer, and R. Knorren, Phys. Rep. **280** (1997) 1.
67. J. M. Lattimer, C. J. Pethick, M. Prakash, and P. Haensel, Phys. Rev. Lett. **66** (1991) 2701.
68. M. Prakash, M. Prakash, J. M. Lattimer, and C. J. Pethick, Astrophys. J. **390** (1992) L77.
69. P. Haensel and O. Yu. Gnedin, Astron. & Astrophys. **290** (1994) 458.
70. Ch. Schaab, F. Weber, M. K. Weigel, and N. K. Glendenning, Nucl. Phys. **A605** (1996) 531.
71. G. Baym, *Neutron Stars and the Physics of Matter at High Density*, in: Nuclear Physics with Heavy Ions and Mesons, Vol. 2, Les Houches, Session XXX, ed. by R. Balian, M. Rho and G. Ripka (North-Holland, Amsterdam, 1978) p. 745.
72. S. Barshay and G. E. Brown, Phys. Lett. **47B** (1973) 107.
73. G. E. Brown, K. Kubodera, D. Page, and P. Pizzochero, Phys. Rev. D **37** (1988) 2042.
74. D. B. Kaplan and A. E. Nelson, Phys. Lett. **175B** (1986) 57; *ibid.* Nucl. Phys. **A479** (1988) 273.
75. G. E. Brown, K. Kubodera, and M. Rho, Phys. Lett. **192B** (1987) 273.
76. C.-H. Lee and M. Rho, *Kaon condensation in dense stellar matter*, Proc. of the International Symposium on Strangness and Quark Matter, ed. by G. Vassiliadis, A. Panagiotou, B. S. Kumar, and J. Madsen (World Scientific, Singapore, 1995) p. 283.
77. R. Barth et al., Phys. Rev. Lett. **78** (1997) 4007.
78. P. Senger, Nucl. Phys. **A685** (2001) 312c.
79. C. Sturm et al., Phys. Rev. Lett. **86** (2001) 39.
80. A. Devismes, J. Phys. G: Nucl. Part. Phys. **28** (2002) 1591.
81. Ch. Fuchs, Prog. Part. Nucl. Phys. **56** (2006) 1.
82. G. Q. Li, C.-H. Lee, and G. E. Brown, Nucl. Phys. **A625** (1997) 372.
83. G. Q. Li, C.-H. Lee, and G. E. Brown, Phys. Rev. Lett. **79** (1997) 5214.
84. G. E. Brown, Phys. Bl. **53** (1997) 671.
85. G. E. Brown, *Supernova Explosions, Black Holes and Nucleon Stars*, in: Proceedings of the Nuclear Physics Conference – INPC '95, ed. by S. Zuxun and X. Jincheng (World Scientific, Singapore, 1996) p. 623.
86. V. Thorsson, M. Prakash, and J. M. Lattimer, Nucl. Phys. **A572** (1994) 693.
87. F.-K. Thielemann, M.-A. Hashimoto, and K. Nomoto, Astrophys. J. **349** (1990) 222.
88. R. L. Jaffe, Phys. Lett. **38** (1977) 195.
89. R. Tamagaki, Prog. Theor. Phys. **85** (1991) 321.
90. T. Sakai, J. Mori, A. J. Buchmann, K. Shimizu, and K. Yazaki, Nucl. Phys. **A625** (1997) 192.
91. N. K. Glendenning and J. Schaffner-Bielich, Phys. Rev. C **58** (1998) 1298.
92. A. Faessler, A. J. Buchmann, M. I. Krivoruchenko, and B. V. Martemyanov, Phys. Lett. **391B** (1997) 255.
93. A. Faessler, A. J. Buchmann, and M. I. Krivoruchenko, Phys. Rev. C **56** (1997) 1576.

94. R. Jaffe and F. Wilczek, Phys. Rev. Lett. **91** (2003) 232003.
95. R. L. Jaffe, Phys. Rep. **409** (2005) 1; Nucl. Phys. Proc. Suppl. **142** (2005) 343.
96. D. D. Ivanenko and D. F. Kurdgelaidze, Astrophys. **1** (1965) 251.
97. N. Itoh, Progr. Theor. Phys. **44** (1970) 291.
98. H. Fritzsch, M. Gell–Mann, and H. Leutwyler, Phys. Lett. **47B** (1973) 365.
99. G. Baym and S. Chin, Phys. Lett. **62B** (1976) 241.
100. B. D. Keister and L. S. Kisslinger, Phys. Lett. **64B** (1976) 117.
101. G. Chapline and M. Nauenberg, Phys. Rev. D **16** (1977) 450.
102. W. B. Fechner and P. C. Joss, Nature **274** (1978) 347.
103. G. Chapline and M. Nauenberg, Ann. New York Academy of Sci. **302** (1977) 191.
104. N. K. Glendenning, Phys. Rev. D **46** (1992) 1274.
105. N. K. Glendenning, S. Pei, and F. Weber, Phys. Rev. Lett. **79** (1997) 1603.
106. A. Chodos, R. L. Jaffe, K. Johnson, C. B. Thorne, and V. F. Weisskopf, Phys. Rev. D **9** (1974) 3471.
107. A. Chodos, R. L. Jaffe, K. Johnson, and C. B. Thorne, Phys. Rev. D **10** (1974) 2599.
108. F. Weber, A. Torres i Cuadrat, A. Ho, and P. Rosenfield, (`astro-ph/0602047`).
109. F. Weber, J. Phys. G: Nucl. Part. Phys. **25** (1999) R195.
110. N. K. Glendenning and F. Weber, *Signal of Quark Deconfinement in Millisecond Pulsars and Reconfinement in Accreting X-ray Neutron Stars*, Lecture Notes in Physics **578**, (Springer-Verlag, Berlin, 2001), p. 305.
111. M. Alford, C. Kouvaris, and K. Rajagopal, Phys. Rev. Lett. **92** (2004) 222001.
112. K. Rajagopal and F. Wilczek, Phys. Rev. Lett. **86** (2001) 3492.
113. P. F. Bedaque and T. Schäfer, Nucl. Phys. **A697** (2002) 802.
114. D. B. Kaplan and S. Reddy, Phys. Rev. D **65** (2002) 054042.
115. M. Buballa, J. Hosek and M. Oertel, Phys. Rev. Lett. **90** (2003) 182002.
116. A. Schmitt, *Spin-one Color Superconductivity in Cold and Dense Quark Matter*, Ph.D. thesis, `nucl-th/0405076`.
117. T. Schäfer, Phys. Rev. D **62** (2000) 094007.
118. M. Alford, J. A. Bowers, and K. Rajagopal, Phys. Rev. D **63** (2001) 074016.
119. J. A. Bowers and K. Rajagopal, Phys. Rev. D **66** (2002) 065002.
120. R. Casalbuoni and G. Nardulli, Rev. Mod. Phys. **76** (2004) 263.
121. M. Alford, K. Rajagopal, and F. Wilczek, Nucl. Phys. **B537** (1999) 443.
122. D. T. Son, Phys. Rev. D **D59** (1999) 094019.
123. M. Alford and S. Reddy, Phys. Rev. D **67** (2003) 074024.
124. M. Alford, J. Phys. G **30** (2004) S441.
125. K. Rajagopal, Acta Physica Polonica B **31** (2000) 3021.
126. M. Alford, J. A. Bowers, and K. Rajagopal, J. Phys. G **27** (2001) 541.
127. D. Blaschke, D. M. Sedrakian, and K. M. Shahabasyan, Astron. & Astrophys. **350** (1999) L47.
128. M. Alford, K. Rajagopal, S. Reddy, and A. W. Steiner, Phys. Rev. D **73** (2006) 114016.
129. J. Madsen, Phys. Rev. Lett. **61** (1988) 2909.
130. G. J. Mathews, I.-S. Suh, B. O'Gorman, N. Q. Lan, W. Zech, K. Otsuki, and F. Weber, J. Phys. G: Nucl. Part. Phys. **32** (2006) 1.
131. Ch. Kettner, F. Weber, M. K. Weigel, and N. K. Glendenning, Phys. Rev. D **51** (1995) 1440.
132. P. Jaikumar, S. Reddy, A. W. Steiner, Phys. Rev. Lett. **96** (2006) 041101.

133. J. L. Provencal, H. L. Shipman, E. Hog, and P. Thejll, Astrophys. J. **494** (1998) 759.
134. J. L. Provencal, H. L. Shipman, D. Koester, F. Wesemael, and P. Bergeron, Astrophys. J. **568** (2002) 324.
135. S. O. Kepler et al., Astrophys. J. **539** (2000) 379.
136. G. J. Mathews, B. O'Gorman, K. Otsuki, I. Suh, and F. Weber, Univ. of Notre Dame preprint (2003).
137. V. V. Usov, Phys. Rev. Lett. **80** (1998) 230.
138. V. V. Usov, Astrophys. J. **550** (2001) L179.
139. V. V. Usov, Astrophys. J. **559** (2001) L137.
140. K. S. Cheng and T. Harko, Astrophys. J. **596** (2003) 451.
141. C. Vogt, R. Rapp, and R. Ouyed, Nucl. Phys. **A735** (2004) 543.
142. F. Weber, M. Meixner, R. P. Negreiros, and M. Malheiro, *Ultra-Dense Neutron Star Matter, Strange Quark Stars, and the Nuclear Equation of State*, (`astro-ph/0606093`).
143. N. K. Glendenning, Phys. Lett. **114B** (1982) 392;
N. K. Glendenning, Astrophys. J. **293** (1985) 470;
N. K. Glendenning, Z. Phys. A **326** (1987) 57;
N. K. Glendenning, Z. Phys. A **327** (1987) 295.
144. L. Lindblom, *Neutron Star Pulsations and Instabilities*, in: Gravitational Waves: A Challenge to Theoretical Astrophysics, edited by V. Ferrari, J. C. Miller, and L. Rezzolla, ICTP Lecture Notes Series, Vol. III, (ISBN 92-95003-05-5, May 2001), (`astro-ph/0101136`).
145. N. Andersson, Astrophys. J. **502** (1998) 708.
146. N. Andersson and K. Kokkotas, Int. J. Mod. Phys. **D10** (2001) 381.
147. L. Lindblom and B. Owen, Phys. Rev. D **65** (2002) 063006.
148. J. L. Friedman and S. M. Morsink, Astrophys. J. **502** (1998) 714.
149. J. Madsen, Phys. Rev. Lett. **81** (1998) 3311.
150. J. Madsen, Phys. Rev. Lett. **85** (2000) 10.
151. M. van der Klis, Ann. Rev. Astron. Astrophys. **38** (2000) 717.
152. C. Manuel, A. Dobado, and F. J. Llanes-Estrada, *Shear Viscosity in a CFL Quark Star*, (`hep-ph/0406058`).
153. V. V. Usov, Phys. Rev. D **70** (2004) 067301.
154. S. Ray, A. L. Espíndola, M. Malheiro. J. P. S. Lemos, and V. T. Zanchin, Phys. Rev. D **68** (2003) 084004.
155. J. D. Bekenstein, Phys. Rev. D **4** (1971) 2185.
156. The AMS home page is `http://ams.cern.ch`.
157. J. Sandweiss, J. Phys. G: Nucl. Part. Phys. **30** (2004) S51.
158. T. Saito, Y. Hatano, Y. Fukuda, and H. Oda, Phys. Rev. Lett. **65** (1990) 2094.
159. T. Saito, *Test of the CRASH experiment counters with heavy ions*, Proc. of the International Symposium on Strangeness and Quark Matter, ed. by G. Vassiliadis, A. D. Panagiotou, B. S. Kumar, and J. Madsen (World Scientific, Singapore, 1995) p. 259.
160. M. Ichimura et al., Nuovo Cimento A **36** (1993) 843.
161. Information about ECCO can be found at `http://ultraman.berkeley.edu`.
162. S. B. Shaulov, APH N.S., Heavy Ion Physics **4** (1996) 403.
163. A. De Rújula, S. L. Glashow, R. R. Wilson, and G. Charpak, Phys. Rep. **99** (1983) 341.
164. O. Miyamura, Proc. of the 24th International Cosmic Ray Conference, 1 (Rome, 1995) p. 890.

165. J. J. Lord and J. Iwai, Paper 515, presented at the International Conference on High Energy Physics, Dallas (1992); H. Wilczynski et al., Proceedings of the XXIV International Cosmic Ray Conference, HE Sessions, Rome (1995), Vol. 1, p. 1.
166. MACRO Collaboration, Phys. Rev. Lett. **69** (1992) 1860.
167. M. Ambrosio et al., EPJ **C13** (2000) 453.
168. M. Ambrosio et al., for the MACRO Collaboration, *Status Report of the MACRO Experiment for the year 2001* , (`hep-ex/0206027`).
169. G. Giacomelli, for the MACRO Collaboration, (`hep-ex/0210021`).
170. Z.-T. Lu, R. J. Holt, P. Mueller, T. P. O'Connor, J. P. Schiffer, and L.-B. Wang, *Searches for Stable Strangelets in Ordinary Matter: Overview and a Recent Example*, (`nucl-ex/0402015`).
171. A. De Rújula and S. L. Glashow, Nature **312** (1984) 734.
172. P. B. Price, Phys. Rev. Lett. **52** (1984) 1265.
173. M. Brügger, K. Lützenkirchen, S. Polikanov, G. Herrmann, M. Overbeck, N. Trautmann, A. Breskin, R. Chechik, Z. Fraenkel, and U. Smilansky, Nature **337** (1989) 434.
174. M. C. Perillo Isaac et al., Phys. Rev. Lett. **81** (1998) 2416; *ibid.* **82** (1999) 2220 (erratum).
175. J. Thomas and P. Jacobs, *A Guide to the High Energy Heavy Ion Experiments*, UCRL-ID-119181.
176. A. Rusek et al., (E886 collaboration), Phys. Rev. C **54** (1996) R15.
177. G. Van Buren (E864 Collaboration), J. Phys. G: Nucl. Part. Phys. **25** (1999) 411.
178. J. Belz et al., (BNL E888 collaboration), Phys. Rev. D **53** (1996) R3487.
179. J. Belz et al., (BNL E888 collaboration), Phys. Rev. Lett. **76** (1996) 3277.
180. F. Dittus et al. (NA52 collaboration), *First look at NA52 data on Pb–Pb interactions at 158 A GeV/c*, International Conference on Strangeness in Hadronic Matter, ed. by J. Rafelski, AIP 340 (American Institute of Physics, New York, 1995) p. 24.
181. G. Appelquist et al., Phys. Rev. Lett. **76** (1996) 3907.
182. G. Ambrosini et al., Nucl. Phys. **A610** (1996) 306c.
183. R. Klingenberg, J. Phys. G: Nucl. Part. Phys. **25** (1999) R273.
184. T. Klahn *et al.*, Phys. Rev. C **74** (2006) 035802.
185. J. Lattimer and M. Prakash, Phys. Rev. Lett. **94** (2005) 111101.
186. M. Alford, D. Blaschke, A. Drago, T. Klahn, G. Pagliara, J. Schaffner-Bielich, Nature 445 (2007) E7, (`astro-ph/0606524`).
187. J. L. Zdunik, P. Haensel, E. Gourgoulhon, and M. Bejger, Astron. & Astrophys. **416** (2004) 1013.
188. E. Chubarian, H. Grigorian, G. Poghosyan, and D. Blaschke, Astron. & Astrophys. **357** (2000) 968.
189. D. Page and V. V. Usov, Phys. Rev. Lett. **89** (2002) 131101.
190. V. V. Usov, Phys. Rev. Lett. **87** (2001) 021101.
191. J. E. Horvath, H. Vucetich, and O. G. Benvenuto, Mon. Not. R. Astron. Soc. **262** (1993) 506.
192. See, for instance, `astro-ph/0207527`.